Automatic alignment of optical interferometers

Euan Morrison, Brian J. Meers, David I. Robertson, and Henry Ward

We present a description of a system for automatic alignment of optical interferometers. The technique relies on using differential phase modulation to permit the detection of the phase difference between two fundamental-mode Gaussian beams at the output of an interferometer. Measurements of the spatially varying phase difference between the two beams by use of one or more multielement photodiodes permits information to be derived about the mismatch in overlap between the phase fronts at the output of the interferometer.

Key words: Alignment, interferometry, Michelson, Fabry–Perot, gravitational wave detectors.

1. Introduction

Laser interferometers typically derive their output signal by detecting the change in the intensity pattern that results when the relative phase of the two interfering beams alters. Maximum sensitivity in such interferometers is obtained only when the relative alignment of the interfering beams is optimized. In many interferometers, particularly ones in which optical components are not rigidly mounted, some automatic method of acquiring and maintaining correct alignment is highly desirable. Ideally the signals for any such system should be derived directly from the interference of the two beams; suitable control signals may then be applied to move components in the interferometer, causing the beams to overlap optimally.

Such a system is particularly attractive in high-precision experiments for which sensitivity is of paramount importance. For example, autoalignment techniques will be of vital importance for the large-scale laser interferometers currently being proposed for the detection of gravitational radiation.[1–3]

2. Misalignment in Two-Beam Interferometers

Consider the simple Michelson interferometer shown in Fig. 1. If the lengths of the two arms are equal, misalignment of mirrors M1, M2, or beam splitter B1 can result only in an angular misalignment of the two output beams.

In a more general interferometer, such as a nonequal path-length Michelson, a Mach–Zehnder, or a resonant cavity used in reflection, it is also possible to introduce purely lateral misalignments between the two interfering beams. This is illustrated in Fig. 2 for the case of a resonant cavity viewed in reflection. The particular cavity shown consists of a plane input mirror and a curved mirror of high reflectivity. The two interfering components can be considered to be the beam that is directly reflected off the front surface of the plane mirror and the beam that is due to the light that leaks out of the cavity when it is on resonance. As can be seen from the diagram, misalignment of the curved rear mirror causes a purely lateral misalignment of the interfering beams.

In general then, the two beams at the output of any interferometer may be both angularly and laterally misaligned in each of two orthogonal directions. Four independent alignment signals must therefore be derived to permit control of all degrees of freedom.

In addition to the angular and lateral misalignments described above, it is also possible for there to be mismatches in the radii of curvature and sizes of the two interfering beams. A further four independent signals must therefore be derived for full determination of first-order errors in the overlap of the two beams.

3. Alignment Techniques

A. Review

One standard method of sensing mismatches is to modulate the mismatch to be determined and coherently detect the resulting intensity change in the interference pattern. For lateral and angular errors, either modulation of the position and angle of the input laser beam with respect to the interferom-

The authors are with the Department of Physics and Astronomy, University of Glasgow, Glasgow G12 8QQ, Scotland.

B. J. Meers is deceased.

Received 7 July 1993; revised manuscript received 15 November 1993.

0003-6935/94/225041-09$06.00/0.

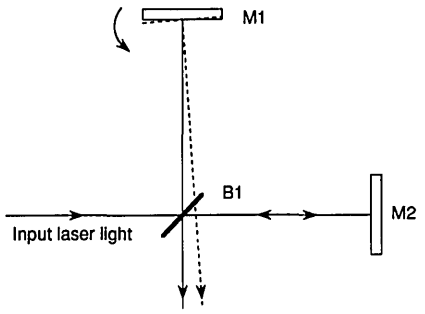

Fig. 1. Effect of misalignment of one of the mirrors in a simple equal path-length Michelson interferometer.

eter components or modulation of the orientations of a suitable number of interferometer mirrors may be used.

Both modulation techniques have been demonstrated on interferometers at the University of Glasgow.[4] Modulation of the pointing direction of the main laser beam was used to derive alignment signals for two 10-m cavities formed between mirrors mounted on suspended masses; feedback systems then optimized the alignment of the cavities. In further experiments modulation of the orientation of interferometer mirrors has also been used to align a small benchtop Michelson system. Such systems have more recently been developed and extensively analyzed at the University of Naples.[5,6]

Although these modulation techniques may be useful in some applications, it is not always desirable or possible to modulate the alignment of what is ideally a mechanically quiet system. Furthermore, if the modulation is to be achieved by mechanical movement of optical components, the imposition of the four modulation frequencies required for full alignment information to be obtained could severely limit the attainable bandwidth of alignment control.

A quite different method, suitable for aligning resonant optical cavities, has been described by Anderson[7] and demonstrated experimentally.[8] This technique relies on using auxiliary phase modulation of the laser light to probe any misalignment-driven susceptibility of the locked cavity to resonate in higher-order spatial modes. Any resulting beat signals in the intensity transmitted through the cavity are detected by a multielement photodiode and coherent demodulation used to derive the required alignment information. Once again the use of additional modulations may be a disadvantage in some applications.

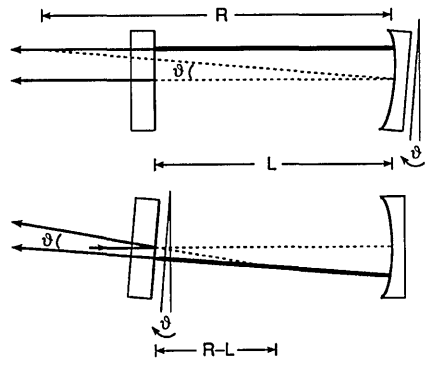

Fig. 2. Effects of misalignment of the two mirrors in a plane/curved cavity of length L in which the radius of curvature of the rear mirror is R. The directly reflected and cavity leakage beams are indicated schematically by the arrowed lines. (The incident beam in each case is propagating horizontally and strikes the plane mirror at its midpoint.) Note that the path followed by the superposition of the two components depends on their relative magnitudes.

B. Alignment with Differential Phase Sensing—an Outline

An alternative technique was suggested some years ago by Drever at the California Institute of Technology,[9] and preliminary experimental tests of the idea were carried out by one of us (Ward) on the prototype gravitational wave detector there. Drever's proposal was to extend the use of the one modulation technique—differential phase modulation—that is normally already employed in applications of high-precision interferometry.[10] In such a system a measure of the phase difference between the two interfering beams is readily obtained from coherent detection of the resulting modulation of the intensity of the interference pattern. The demodulated signal may then be used to lock the interferometer to the desired operating point, frequently a null of intensity at the detected output. The extension to this technique is to make spatially sensitive measurements of the intensity modulation in the interference pattern to derive information about all possible mismatches of overlap of the two interfering beams. Such a system has recently been implemented on one of the 10-m-long suspended optical cavities in the Glasgow prototype gravitational wave detector. The results of this test are described in detail in Ref. 11.

As an illustration consider a simple angular misalignment α between two interfering beams, one of which has been phase modulated. To simplify the picture, consider for the moment only what happens at the beam waist (i.e., where the phase fronts of the two beams are plane). Also, let us assume that the interferometer output is maintained on a null, possibly by some servo system. If we look at the phase fronts, we therefore see that while the overall phase difference between the two beams is π, the misalignment has introduced a differential phase gradient across the interference pattern. Now consider looking at the output with a split photodiode. Assuming that equal intensities fall on the two halves of the photodiode, the phase difference deduced from the signal detected by one half is $\pi + \phi$, whereas the phase difference deduced from the other half of the photodiode is $\pi - \phi$, where ϕ is proportional to the misalignment α. If these two results are subtracted, the resulting signal is directly proportional to the angular misalignment of the two beams.

One simple method of sensing a translational misalignment between the two beams is to place a suitable lens before the detecting photodiode. The

lens can be chosen so that a differential phase gradient occurs near its focal plane; this phase gradient may be sensed as before. (This topic is more fully discussed in Subsection 5.B.)

In an analogous manner errors in beam curvature and size may in principle be detected with photodetectors in which separate signals are derived from a central section and from a surrounding annular region.

This scheme has the considerable advantage that no further modulation need be applied to the interferometer. Any interferometer that is locked by differential phase sensing can be aligned with this technique.

Before proceeding to a detailed discussion it is appropriate to introduce the mathematical framework of a mode description of propagating laser beams. This introduction is followed by a discussion of the types of mismatch possible in a two-beam interferometer and of how they may be sensed.

4. General Misalignments

A. Expansion of Laser Beams in Terms of Orthogonal Modes of Propagation

For a full description of first-order errors it is convenient to introduce an orthogonal set of modes of propagation that can be used to expand any given electric-field distribution. For simplicity we restrict our discussion to cases in which the errors of alignment are confined to a single transverse direction; extension to the orthogonal dimension is straightforward. Following the notation of Kogelnik and Li,[12] in a Cartesian coordinate system we may write the nth- order mode of a beam propagating in the positive direction along the z axis as

$$U_n(x, z) = N_n H_n\left(\sqrt{2}\,\frac{x}{\omega}\right)\frac{\omega_0}{\omega} \times \exp\left[-j(kz - \phi_n) - x^2\left(\frac{1}{\omega^2} + \frac{jk}{2R}\right)\right], \quad (1)$$

where x is the distance from the z axis, H_n is the Hermite polynomial of order n, N_n is a normalizing factor, $k = 2\pi/\lambda$, and the additional term ϕ_n that describes the phase difference between the Gaussian beam and an ideal plane-wave approximation is given by

$$\phi_n = (n + 1)\arctan\left(\frac{\lambda z}{\pi\omega_0{}^2}\right). \quad (2)$$

The normalizing factor is often chosen (see, e.g., Boyd and Gordon[13]) to be

$$N_n = \frac{\Gamma\left(\frac{n}{2} + 1\right)}{\Gamma(n + 1)}, \quad (3)$$

which makes $U_n(0, 0) = \pm 1$ for n even and $U_n(0, 0) =$ 0 for n odd. The origin, $z = 0$, is at the location of the beam waist, at which point the beam half-width is ω_0. As the beam propagates, the half-width ω is given by

$$\omega^2 = \omega_0{}^2\left[1 + \left(\frac{\lambda z}{\pi\omega_0{}^2}\right)^2\right] \quad (4)$$

and the beam radius of curvature R is given by

$$R = z\left[1 + \left(\frac{\pi\omega_0{}^2}{\lambda z}\right)^2\right]. \quad (5)$$

At $z = 0$ the fundamental and first two higher-order modes may thus be written as

$$U_0(x) = \exp(-x^2/\omega_0{}^2), \quad (6)$$

$$U_1(x) = (2\pi)^{1/2}\frac{x}{\omega_0}\exp(-x^2/\omega_0{}^2), \quad (7)$$

$$U_2(x) = \left(\frac{4x^2}{\omega_0{}^2} - 1\right)\exp(-x^2/\omega_0{}^2). \quad (8)$$

These results are used in the following subsections, in which for conciseness $U_n(x)$ is written as U_n.

B. Mode Description of Beam Mismatches

To keep the following discussion general and applicable to any differentially phase-modulated two-beam interferometer, we choose as our reference frame a coordinate system with its z axis collinear with the beam that has been modulated; this beam is taken as being in the fundamental mode. Its electric field at the position of the beam waist ($z = 0$) may therefore be written as $E_1 = A_1U_0$. The electric field E_2 of the other interferometer beam may be expanded as a linear combination of the modes U_n, and, provided that the mismatch between the two beams is small, only the first two higher-order modes need normally be considered. For convenience, in this subsection, we include only the spatially dependent parts in our discussion of the electric fields. The treatment is similar to that of Rüdiger *et al.*[14]

1. *Beam Tilts*

If beam 2, initially of the form $E_2 = A_2\exp(-x^2/\omega_0{}^2) = A_2U_0$, is tilted at a small angle α with respect to beam 1 in the direction of the x axis, E_2 may be expressed as

$$E_2 = A_2\exp(-x^2/\omega_0{}^2)\exp(jk\alpha x), \quad (9)$$

which for small values of α can be approximated as

$$E_2 \simeq A_2\left[U_0 + j\frac{k\omega_0}{(2\pi)^{1/2}}\alpha U_1\right]. \quad (10)$$

It can be seen that tilting a beam that is in the fundamental mode causes a coupling into the first-order mode that is 90° out of phase with the fundamental.

2. Beam Displacements

If beam 2 is laterally offset in the positive x direction by a small amount a,

$$E_2 = A_2 \exp[-(x - a)^2/\omega_0^2], \tag{11}$$

which can be expanded to the form

$$E_2 \simeq A_2\left[U_0 + \left(\frac{2}{\pi}\right)^{1/2}\frac{a}{\omega_0}U_1\right]. \tag{12}$$

A lateral offset is thus equivalent to the in-phase addition of a first-order mode term.

3. Waist-Position Mismatches

An error in beam curvature will arise if the waist position of beam 2 is displaced by a small amount b along the z axis from the waist position of beam 1 at $z = 0$. If we assume that the waist sizes in the x direction are both ω_0, the reciprocal of the radius of curvature of beam 2 at $z = 0$ differs slightly from zero and is given by

$$\frac{1}{R_2} = \frac{1}{-b\left[1 + \left(\frac{\pi\omega_0^2}{\lambda b}\right)^2\right]}. \tag{13}$$

The electric field of beam 2 at $z = 0$ can be written as

$$E_2 = A_2 \exp\left(-\frac{x^2}{\omega_0^2} - j\frac{x^2 k}{2R_2}\right). \tag{14}$$

Expanding the exponential and simplifying yield the approximation

$$E_2 \simeq A_2\left[U_0 - j\frac{k\omega_0^2}{8R_2}\{U_2 + U_0\}\right], \tag{15}$$

which, provided $b \ll \pi\omega_0^2/\lambda$, can be expressed as

$$E_2 \simeq A_2\left[U_0 + j\frac{b}{2k\omega_0^2}\{U_2 + U_0\}\right]. \tag{16}$$

A curvature mismatch is thus represented by a coupling into the second-order mode that is 90° out of phase with the fundamental. A full description of a curvature mismatch would have an equivalent term in the expansion in the y direction.

4. Waist-Size Mismatches

The final form of mismatch to be considered is that of an error in beam size. Consider the case in which beam 2 has a waist size in the x direction that differs by a small amount $\Delta\omega$ from that of beam 1. Then

$$E_2 = A_2 \exp[-x^2/(\omega_0 + \Delta\omega)^2], \tag{17}$$

which may be expanded and simplified to

$$E_2 \simeq A_2\left[U_0 + \frac{\Delta\omega}{2\omega_0}\{U_2 + U_0\}\right] \simeq A_2\left[U_0 + \frac{\Delta\omega}{2\omega_0}U_2\right]. \tag{18}$$

A waist-size mismatch can thus be described as an in-phase addition of a second-order mode term. Once again a full description of a size mismatch would have an equivalent term in the expansion in the y direction.

5. Summary

The errors considered are all simply described as inphase or quadrature couplings into the first- or second-order spatial modes. We now have to consider how signals proportional to these mismatches can be deduced from observations of the interference between the two electric fields E_1 and E_2.

5. Signal Detection

To simplify the following analysis it is convenient to express the nth-order mode of a beam propagating along the positive z axis [given by Eq. (1)] as

$$U_n(x, z) = \mathscr{U}_n(x, z)\exp[j\varphi_n(z)], \tag{19}$$

where

$$\mathscr{U}_n(x, z) = N_n H_n\left(\sqrt{2}\frac{x}{\omega}\right)\frac{\omega_0}{\omega} \times \exp\left[-j(kz - \phi_0) - x^2\left(\frac{1}{\omega^2} + \frac{jk}{2R}\right)\right] \tag{20}$$

and $\varphi_n(z)$ is the phase difference that evolves between the fundamental and the nth mode as the beams propagate along the z axis. From Eq. (2) it follows that

$$\varphi_n(z) = n \arctan\left(\frac{\lambda z}{\pi\omega_0^2}\right). \tag{21}$$

For conciseness $\mathscr{U}_n(x, z)$ will be written as $\mathscr{U}_n$. Note that at the beam waist $\mathscr{U}_n = U_n$.

We will define beam 1 to be given by $E_1 = A_1 a_0 \mathscr{U}_0$, where the complex number a_0 includes the time dependence of the field, the effect of the differential phase modulation, and any static phase difference with respect to the fundamental-mode component of beam 2. If the phase modulation is given by $m(t)$, a_0 can be written as

$$a_0 = \exp\{j[\omega t + m(t) + \Phi]\}, \tag{22}$$

where ω is the angular frequency of the light and Φ is the relative phase difference between the fundamental-mode components of the two beams.

Similarly we can write the unmodulated but mismatched beam as

$$E_2 = A_2(b_0\mathscr{U}_0 + b_1\mathscr{U}_1 + b_2\mathscr{U}_2). \tag{23}$$

where the coefficients b_n are complex and depend on the type and magnitude of the mismatch between the two beams and also on the distance z from the waist position of beam 1. The coefficients b_n can be written in a general way as

$$b_n = r_n \exp(j\theta_n)\exp\{j[\omega t + \varphi_n(z)]\}, \quad (24)$$

where r_n and θ_n are determined by the mismatches.

For the four mismatches considered above we have already seen that in all cases $r_0 \sim 1$ and $\theta_0 = 0$. We have also seen that for errors in tilt, $\theta_1 = \pi/2$, and in translation, $\theta_1 = 0$; in both these cases $r_1 \ll 1$ and $r_2 = 0$. For errors in the waist position, $\theta_2 = \pi/2$, and in the waist size, $\theta_2 = 0$, with $r_1 = 0$ and $r_2 \ll 1$ in both cases.

It is now straightforward to compute the resulting interference pattern. The resultant field E is given by

$$E = E_1 + E_2 = (a_0A_1 + b_0A_2)\mathscr{U}_0 + b_1A_2\mathscr{U}_1 + b_2A_2\mathscr{U}_2, \quad (25)$$

and the intensity may be obtained from $EE^\star$.

Coherent detection at the modulation frequency is used to process the signals from photodiodes looking at the interference pattern, and therefore only terms in the expansion of $EE^\star$ that contain a_0 or $a_0^\star$ can contribute. Extracting such terms gives

$$\begin{aligned}[EE^\star]_{\text{mod}} = {} & \mathscr{U}_0^2A_1A_2(b_0a_0^\star + b_0^\star a_0) \\ & + \mathscr{U}_0\mathscr{U}_1A_1A_2(b_1a_0^\star + b_1^\star a_0) \\ & + \mathscr{U}_0\mathscr{U}_2A_1A_2(b_2a_0^\star + b_2^\star a_0). \end{aligned} \quad (26)$$

The terms of the form $(b_na_0^\star + b_n^\star a_0)$ can be written as

$$(b_na_0^\star + b_n^\star a_0) = 2r_n\cos\{m(t) + [\Phi - \theta_n - \varphi_n(z)]\}, \quad (27)$$

which can be expanded to the form

$$2r_n[\cos m(t)\cos\Psi_n + \sin m(t)\sin\Psi_n], \quad (28)$$

where $\Psi_n = [\Phi - \theta_n - \varphi_n(z)]$. If we assume a small modulation depth ($|m(t)| \ll 1$), the component at the modulation frequency is simply proportional to $r_n\, m(t)\sin\Psi_n$.

From Eq. (26) it is clear that there are several components of the resultant field that can contain spatially dependent intensity modulation. The signal produced when the interference pattern is incident on a photodetector is thus a function of the overlap of the pattern with the detector area.

A. Detection with a Single Photodiode

The modulated light intensity I_m that results when the combined beam is incident on a single photodetector is proportional to the integral of $[EE^\star]$ over the photodiode area. Provided the detector area is large compared with the beam size, the limits of integration are effectively $\pm\infty$. (In our one-dimensional treatment the integral is simply evaluated along the x axis.) The orthogonality of the modes of propagation ensures that no net contribution to the integral results from terms involving $\mathscr{U}0\mathscr{U}_1$ or $\mathscr{U}_0\mathscr{U}_2$. The modulated intensity may thus be expressed as

$$I_m \propto m(t)A_1A_2\sin\Phi. \quad (29)$$

For maximum sensitivity to small changes in Φ the interferometer path difference is normally adjusted so that the mean value of Φ is a multiple of π rads. The optimum signal-to-noise ratio is obtained when this condition is met and when the standing light power on the photodetector is at a minimum, so in practice an interferometer is usually locked on a null fringe for which $\Phi = \pi$, a condition that will be assumed in the following discussions. This approach is simply the conventional differential phase-modulation technique for obtaining an error signal proportional to small offsets from the null setting.

B. Detection with a Rectangularly Split Photodiode

Consider now the result of using a split photodetector divided along the y axis to view the interference pattern. (Again we assume that the photodetector area is large compared with the beam size.) If the combined beam is incident symmetrically on the split photodiode and if the outputs of the two detectors are differenced, the effective modulated light intensity I_m can be deduced from

$$I_m \propto \int_0^\infty [EE^\star]dx - \int_{-\infty}^0 [EE^\star]dx. \quad (30)$$

Only odd functions can provide a net contribution, so

$$I_m \propto r_1m(t)A_1A_2\sin\Psi_1 = r_1m(t)A_1A_2\sin[\theta_1 + \varphi_1(z)], \quad (31)$$

where [from Eq. (21)] $\varphi_1(z) = \arctan[\lambda z/(\pi\omega_0^2)]$.

In general therefore the demodulated signal will be a measure of some combination of tilt and translational errors. It is straightforward to see that the signal resulting from a given tilt error ($\theta_1 = \pi/2$) will be proportional to $\cos[\varphi_1(z)]$, giving a maximum response at the position of the waist ($z = 0$), whereas the signal produced by a translational error ($\theta_1 = 0$) will be proportional to $\sin[\varphi_1(z)]$, yielding maximum sensitivity in the far field ($z \gg \pi\omega_0^2/\lambda$) where $\varphi_1(z) \to \pi/2$.

These results may be understood from simple geometrical considerations.

For the case of an angular misalignment it is clear that a signal is readily detectable at the location of the beam waist where the phase fronts are plane. However, as the beams propagate to a large distance $d \gg \pi\omega_0^2/\lambda$ from the waist, the radius of curvature of the phase fronts will approximate d for both beams. There will thus be no phase gradient across the combined beam, and hence no signal will result.

A lateral offset of one beam will cause no phase gradient at the position of the beam waists, and hence no signal will result from a split photodiode measurement at that location. At large distances from the waist the phase fronts of the two beams will have the same curvature, but because of the lateral displacement the phase fronts of one beam will exhibit a net lead above the x axis, whereas below the axis they will lag. Detection with a split photodiode therefore yields a signal. In the far-field region the curvature of the phase fronts decreases linearly with z ($R \simeq z$), and it is straightforward to show that the phase difference between the two beams at a point on the phase front that subtends an angle β at the origin of the z axis tends to a constant value as z increases. Also the beam width increases linearly with z, and so the power in a small angle $\Delta\beta$ around β is constant. Hence in the far field the signal size becomes almost independent of distance along the z axis.

C. Detection with an Annularly Split Photodiode

Consider now detecting the interference pattern with a split diode comprising a circular center region of radius r and a separate surrounding annular region. If the combined beam is centered and if the signals from the two sections are differenced, then in our one-dimensional example the effective modulated light intensity will be given by

$$I_m \propto \int_{-\infty}^{-r} [EE^\star]dx + \int_r^\infty [EE^\star]dx - \int_{-r}^{r} [EE^\star]dx, \quad (32)$$

provided the outer radius of the annular region is much greater than the beam half-width.

From symmetry considerations, only even functions appearing in $EE^\star$ can provide a net contribution. It thus follows that

$$I_m \propto r_2 m(t) A_1 A_2 \sin \Psi_2 = r_2 m(t) A_1 A_2 \sin [\theta_2 + \varphi_2(z)], \quad (33)$$

where

$$\varphi_2(z) = 2 \arctan\left(\frac{\lambda z}{\pi {\omega_0}^2}\right). \quad (34)$$

Here it is clear that the demodulated signal will have a maximum response to a beam curvature mismatch ($\theta_2 = \pi/2$) at the position of the waist of the reference beam and also when $z \gg \pi{\omega_0}^2/\lambda$. Sensitivity of the measurement to an error in relative waist size ($\theta_2 = 0$) will be at a maximum when $\varphi_2(z) = \pi/2$, which occurs when $z = \pi{\omega_0}^2/\lambda$.

Once again these results may be understood from simple physical arguments.

A signal can be detected only when the curvatures of the phase fronts at the position of the split photodiode are different. When there is a small mismatch in curvature it is clear that the split diode will respond when placed at the waist of the reference beam. As the two beams propagate, however, there is always a value of z at which they will have the same curvature and hence a position at which the differential measurement will yield no signal. It is straightforward to show from Eq. (5) that if the relative waist displacement is b, the curvatures are equal when $z = [\pm\pi{\omega_0}^2/\lambda + b/2]$. As $z \to \infty$ the curvatures will always be different and a signal will once again become detectable.

If the original mismatch is in beam size, there is clearly no signal detectable if the split photodiode is placed at the (common) waist position. As the beams propagate, they expand at different characteristic rates, and hence their curvatures become different giving rise to a detectable signal. As $z \to \infty$ the two radii of curvature both tend to z, reducing the detection sensitivity for this kind of error to zero. The maximum response therefore occurs at an intermediate distance.

When using this type of split photodiode, we must take some care to choose the dimensions of the diode segments to suit the size of the beam. The relevant integral that determines the signal coupling is

$$\int_r^\infty \mathcal{U}_0\mathcal{U}_2 dx - \int_0^r \mathcal{U}_0\mathcal{U}_2 dx. \quad (35)$$

Since $\mathcal{U}_0\mathcal{U}_2 = (4x^2/\omega^2 - 1)\exp(-2x^2/\omega^2)$, the largest signal will result when $\int_r^\infty$ is maximally positive and $\int_0^r$ is maximally negative, which will occur when $4r^2/\omega^2 = 1 \Rightarrow r = \omega/2$. Numerical integration shows that greater than 70% of the maximum possible signal will be obtained provided $\omega/4 \le r \le 3\omega/4$.

D. Positional Offsets of Photodiodes

It is important to consider the effect on the various error signals of small movements of the interference pattern away from the symmetrical positions on the detection photodiodes. When a single photodiode is used, there is negligible dependence of the error signal provided the photodiode response is uniform and the beam remains within its active area. However, one might expect some variation in the error signals derived with rectangularly and annularly split photodiodes.

Consider the signal sensed with a rectangularly split photodiode. If the photodiode is offset a small amount d from the center of the interference pattern, we have

$$I_m \propto \int_0^\infty [EE^\star]dx - \int_0^d [EE^\star]dx - \left(\int_{-\infty}^0 [EE^\star]dx + \int_0^d [EE^\star]dx\right), \quad (36)$$

which can be rewritten as

$$I_m \propto m(t)\left[r_1A_1A_2\left(\int_0^\infty \mathscr{U}_0\mathscr{U}_1 dx - \int_0^d \mathscr{U}_0\mathscr{U}_1 dx\right) - r_2A_1A_2\int_0^d \mathscr{U}_0\mathscr{U}_2 dx\right], \quad (37)$$

where it has been assumed that the term involving $\int_0^d \mathscr{U}_0^2 dx$ has been driven to zero by a servo system controlling the path difference between the interfering beams.

The introduction of an offset in the position of the photodiode is thus seen to cause a small reduction in the size of the signal detected that is due to an angular or lateral misalignment together with the coupling in of a small amount of signal proportional to mismatches in beam curvature and size.

Similarly, when an annularly split photodiode is used, the signal detected from beam curvature and size mismatches will be slightly reduced by a positional offset of the photodiode, and a small amount of signal from any angular or lateral misalignments will couple in.

However, provided in each case that the desired signal dominates the contaminating one, optimum alignment will be achieved once servos for all degrees of freedom (angular and lateral misalignments and mismatches in the beam curvature and size) are simultaneously operative.

E. Information Derived from the First Harmonic of the Modulation Frequency

Another important point is that in principle it is possible to use the first harmonic of the modulation frequency to determine full alignment information from a single multielement photodiode. As an example consider the use of a rectangularly split photodiode to determine the lateral and angular offsets of the interfering beams. If we go back to expression (30) and retain the original for the detected intensity given by expression (28), the signal obtained by differencing iating between the outputs of two halves of the split photodiode is given by

$$I_m \propto r_1A_1A_2[\cos m(t) \cos \Psi_1 + \sin m(t) \sin \Psi_1]. \quad (38)$$

If we expand $\cos m(t)$, we see that we obtain terms at twice the modulation frequency since $\cos m(t) \simeq 1 - \frac{1}{2}m^2(t)$ for small modulation depths, and hence one can obtain information that is orthogonal to that derived from the signal detected at the modulation frequency by looking at the component of the intensity at twice the modulation frequency. One could therefore in principle gain full alignment information about the angular and lateral offsets of the two beams using a single multielement photodiode. This technique could also be extended to permit the detection of beam size and curvature mismatches with a single multielement photodiode. In practice, however, small offsets of the photodiode with respect to the interference pattern would permit other signals to couple in at twice the modulation frequency, in particular that which is proportional to $\mathscr{U}_0^2$. Since we are considering small misalignments of the interfering beams, this term is liable to dominate those present at the first harmonic, even for small offsets of the split photodiode.

One possible solution to this problem would be to use some kind of multielement detector such as a CCD array or a scanning camera to map the amplitudes of the fundamental and first harmonic intensity modulation over the beam profile. Computer analysis of the resulting data could then produce the required signals. However, the size of the signal obtained from observations at the first harmonic will be intrinsically small since it is proportional to $|m^2(t)|$, where $|m(t)|$ is typically $\ll 1$. Together with its inherent complexity this relative insensitivity may limit the applicability of this approach.

F. Use of Lenses

We have shown that one can detect relative lateral offsets and errors in beam size using the differential phase-sensing technique by placing split photodiodes at suitable distances from the beam waist. The propagation from the beam waist introduces the required phase shift between the fundamental and the first- and second order modes.

However, for relatively large beam waists, obtaining the necessary phase shift may require placing a photodiode several meters away from the waist. For example, for $\omega_0 = 10^{-3}$ m and $\lambda = 514$ nm, one must place the photodiode ~ 5 m from the waist to detect $\sim 50\%$ of the maximum signal possible arising from a lateral offset.

It is possible to shorten this path length by placing a system of lenses close to the original waist and viewing the interference pattern after the lenses. To illustrate the technique, we will concentrate on a lens system that will provide sensitivity to lateral offsets, i.e., one that causes a phase shift between the fundamental and first-order modes of 90° to develop over a reasonably compact distance. It is also possible, by choosing phase shifts other than 90°, to generate any linear combination of lateral and angular offset signals. A similar approach can be used to design a system suitable for sensing errors in relative beam size, where it is the phase difference between the fundamental and second-order modes that must be made close to 90°.

1. *Use of a Single Lens*

If a single lens is used of power P_1, it is straightforward to show that a new waist of size ω_1 is formed a distance d_1 after the lens where

$$\omega_1^2 = \frac{\omega_0^2}{\left(1 + \frac{P_1^2\pi^2\omega_0^4}{\lambda^2}\right)}, \quad (39)$$

$$d_1 = \frac{1}{P_1\left(1 + \frac{\lambda^2}{P_1^2\pi^2\omega_0^4}\right)}. \quad (40)$$

The phase difference $\varphi_{\omega_0\to\omega_1}$ between the fundamental and first-order modes that accumulates over the distance d_1 can then be expressed as

$$\varphi_{\omega_0\to\omega_1} = -\arctan\left(\frac{d_1\lambda}{\pi\omega_1^2}\right) = -\arctan\left(\frac{P_1\pi\omega_0^2}{\lambda}\right). \quad (41)$$

To achieve the phase difference of 90° needed to make a measurement sensitive to lateral offsets, one strategy would be to choose $P_1 \gg \lambda/(\pi\omega_0^2)$ and to place a photodiode at the waist formed by the lens. The practical difficulty that may be encountered is that, if the lens power is chosen to be large enough to produce a waist a conveniently short distance away, the beam size at the photodetector may be unusably small.

2. *Multiple-Lens Solution*

In such a case a solution in which an extra lens is used may be useful. One approach is to use an additional high-power lens to transform the small waist ω_1 produced by the first lens to another small waist ω_2. In transforming ω_1 to ω_2, a phase shift between the fundamental and first-order modes can be acquired over a compact distance. The beam can then be allowed to expand from ω_2 to a size suitable for use with a quadrant photodiode. Since in this expansion region an extra phase shift of $\sim 90°$ will be accumulated (which is approximately equal and opposite the original phase shift acquired when contracting ω_0 to ω_1), the net phase shift through the whole system will be close to that which is due to the imaging of ω_1 to ω_2.

To illustrate this, consider the system shown in Fig. 3. The first lens is placed (as in the case of the single-lens solution) at the location of the original beam waist and forms the first small waist ω_1 at a distance d_1 as before. The second lens of power $P_2 \gg P_1$ is placed at the position of the waist produced by the first lens.

Using Eqs. (39) and (40) together with the equivalent results for ω_2^2 and d_2, we can show that the net phase shift between the fundamental and first-order modes as the beam propagates from the position of waist ω_1 to that of waist ω_2 is given by

$$\varphi_{\omega_1\to\omega_2} = -\arctan\left(\frac{d_2\lambda}{\pi\omega_2^2}\right) = -\arctan\left(\frac{\gamma P_2}{P_1^2 + \gamma^2}\right), \quad (42)$$

where for convenience we have set $\gamma = \lambda/(\pi\omega_0^2)$. Since the first lens would be chosen so that $P_1 \gg \gamma$, the phase shift may be approximated by

$$\varphi_{\omega_1\to\omega_2} \sim -\arctan\left(\frac{P_2\lambda}{P_1^2\pi\omega_0^2}\right), \quad (43)$$

and this will approximate the phase shift through the whole system provided the distance from ω_2 to the plane of detection is $\gg \pi\omega_2^2/\lambda$. A suitable choice of P_1 and P_2 can thus yield both a compact system and one in which the beam size is suitable for use with typical split photodiodes.

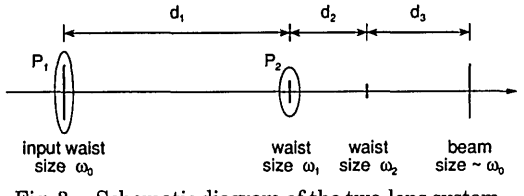

Fig. 3. Schematic diagram of the two-lens system.

G. Shot-Noise-Limited Sensitivity of the Technique

The shot noise limit to the sensitivity of differential phase modulation as a technique for sensing the phase difference between two interfering beams has been discussed by Niebauer *et al.*[15] and by Meers and Strain.[16] Using their results, we see that the shot-noise-limited signal-to-noise ratio for a small signal s, representing a phase difference between two interfering beams, and for a laser power I_0, is given by

$$s\left(\frac{I_0F^2}{2\hbar\omega_L\Delta f}\right)^{1/2}, \quad (44)$$

where F is determined by the efficiency of the modulation/demodulation scheme and can take a value in the range $0 \to 1$.

For example, if we consider an angular misalignment α of the two beams, we can substitute for the signal s the equation $s = k\omega_0\alpha/(2\pi)^{1/2}$ [see approximation (10)], giving a limit to the sensitivity of the detection technique of

$$\alpha > \left(\frac{\hbar\omega_L\lambda^2\Delta f}{I_0\omega_0^2\pi F^2}\right)^{1/2}. \quad (45)$$

For example, if $I_0 = 10^{-3}$ W, $\omega_0 = 10^{-3}$ m, $\lambda = 514$ nm, and if $F = (2/3)^{1/2}$ corresponding to the case of sinusoidal modulation and demodulation,[15,16] the resulting shot noise limit is $\alpha > 7 \times 10^{-12}$ rad/(Hz)$^{1/2}$.

For a lateral offset a between the two beams, we can substitute for s the equation $s = (2/\pi)^{1/2}a/\omega_0$ [see approximation (12)], which gives a shot noise limit of

$$a > \left(\frac{\omega_0^2\pi\hbar\omega_L\Delta f}{I_0F^2}\right)^{1/2}. \quad (46)$$

Using the parameters given above gives $a > 4 \times 10^{-11}\ \mathrm{m/(Hz)^{1/2}}$.

Similar calculations can be performed to estimate the shot noise limit for detecting beam curvature and size mismatches. The calculation may also be extended to include the case of alignment of the mirrors in a resonant optical cavity by suitably modifying the factor F according to the characteristics of the cavity (see Ref. 15).

6. Summary

We have shown how a differential phase-modulation scheme, used to determine the phase difference between two interfering beams at the output of an interferometer, can be extended to give full information about possible misalignments between the beams. Once detected, these signals can be fed back to control the orientation or position of components within the interferometer to ensure optimal alignment.

We thank our colleagues in the Gravitational Waves Research group for their interest in this research, which was supported by the Science and Engineering Research Council and the University of Glasgow. We also thank R. W. P. Drever for suggesting the technique originally and for many useful and stimulating discussions. H. Ward thanks the California Institute of Technology for support while a Visiting Associate in 1984/85 and the Laser Interferometer Gravitational-Wave Observatory (LIGO) project at the California Institute of Technology for support on subsequent visits.

References

1. R. E. Vogt, A. Abramovici, W. Althouse, R. Drever, Y. Gürsel, S. Kawamura, F. Raab, D. Shoemaker, L. Sievers, R. Spero, K. Thorne, R. Weiss, S. Whitcomb, and M. Zucker, in "The U.S. LIGO project," *Proceedings of the Sixth Marcell Grossmann Meeting on General Relativity*, H. Sato and T. Nakamura, eds. (World Scientific, Singapore, 1992), pp. 244–266.
2. A. Giazotto, A. Brillet, C. Bradaschia, R. Del Fabbro, A. Di Virgilio, H. Kautzky, V. Montelatici, D. Passuello, F. Barone, L. Di Fiore, L. Milano, G. Russo, S. Solimeno, M. Capozzi, M. Longo, M. Lops, I. Pinto, G. Rotoli, F. Fuligni, V. Iafolla, G. Natale, O. Cregut, P. Hello, C. N. Man, P. T. Manh, A. Marraud, D. Shoemaker, J-Y. Vinet, J. M. Aguirregabiria, H. Bel, J-P. Duruisseau, G. Le Denmat, P. Tourrenc, T. Damour, S. Bonazzola, J. A. Marck, Y. Gourghoulon, and L. E. Holloway, "The VIRGO project" (INFN, Pisa; Italy; 1989).
3. K. Danzmann, J. Chen, P. G. Nelson, T. M. Niebauer, A. Rüdiger, R. Schilling, L. Schnupp, K. A. Strain, H. Walther, W. Winkler, J. Hough, A. M. Campbell, C. A. Cantley, J. E. Logan, B. J. Meers, E. Morrison, D. I. Robertson, N. A. Robertson, S. Rowan, K. D. Skeldon, P. J. Veitch, H. Ward, H. Welling, P. Aufmuth, I. Kröpke, D. Ristau, J. E. Hall, J. R. J. Bennet, I. F. Corbett, B. W. H. Edwards, R. J. Elsey, R. J. S. Greenhalgh, B. F. Schutz, D. Nicholson, R. J. Shuttleworth, J. Ehlers, P. Kafka, G. Schäfer, H. Braun, and V. Kose, "The GEO project: a long baseline laser interferometer for the detection of gravitational waves," in *Relativistic Gravity Research with Emphasis on Experiments and Observations,* J. Ehlers and G. Schäfer, eds., Lecture Notes in Physics **410** (Springer-Verlag, Berlin, 1992), pp. 184–209.
4. B.J. Meers, "An automatically aligning optical cavity," (University of Glasgow, Glasgow, Scotland, 1985).
5. S. Solimeno, F. Barone, C. de Lisio, L. Di Fiore, L. Milano, and G. Russo, "Fabry–Perot resonators with oscillating mirrors,' Phys. Rev. A **43**, 6227–6240 (1991).
6. F. Barone, L. Di Fiore, L. Milano, G. Russo, and S. Solimeno, "Automatic alignment of a Michelson interferometer," IEEE Trans. Nucl. Sci. **39**, 232–237 (1992).
7. D. Z. Anderson, "Alignment of resonant optical cavities," Appl. Opt. **23**, 2944–2949 (1984).
8. N. M. Sampas and D. Z. Anderson, "Stabilization of laser beam alignment to an optical resonator by heterodyne detection of off-axis modes," Appl. Opt. **29**, 394–403 (1990).
9. R. W. P. Drever, Department of Physics, California Institute of Technology, Pasadena, Calif. 91125 (personal communication, 1984).
10. R. W. P. Drever, J. L. Hall, F. W. Kowalski, J. Hough, G. M. Ford, A. J. Munley, and H. Ward, "Laser phase and frequency stabilization using an optical resonator," Appl. Phys. B **31**, 97–105 (1983).
11. E. Morrison, B. J. Meers, D. I. Robertson, and H. Ward, "Experimental demonstration of an automatic alignment system for optical interferometers," Appl. Opt. **33,** (1994).
12. H. Kogelnik and T. Li, "Laser beams and resonators," Appl. Opt. **5**, 1550–1567 (1966).
13. G. D. Boyd and J. P. Gordon, "Confocal multimode resonator for millimeter through optical wavelength masers," Bell Syst. Tech. J. **40**, 489–508 (1961).
14. A. Rüdiger, R. Schilling, L. Schnupp, W. Winkler, H. Billing, and K. Maischberger, "A mode selector to suppress fluctuations in laser beam geometry," Opt. Acta **28**, 641–658 (1981).
15. T. M. Niebauer, R. Schilling, K. Danzmann, A. Rüdiger, and W. Winkler, "Nonstationary shot noise and its effect on the sensitivity of interferometers," Phys. Rev. A **43**, 5022–5029 (1991).
16. B. J. Meers and K. A. Strain, "Modulation, signal and quantum noise in interferometers," Phys. Rev. A **44**, 4693–4703 (1991).